PLOS ONE

RESEARCH ARTICLE

Valorization of khat (*Catha edulis*) waste for the production of cellulose fibers and nanocrystals

Tesfaye Gabriel*, Kebede Wondu, Jemal Dilebo

Department of Pharmaceutics and Social Pharmacy, School of Pharmacy, College of Health Sciences, Addis Ababa University, Addis Ababa, Ethiopia

* tesfaye.gabriel@aau.edu.et

Citation: Gabriel T, Wondu K, Dilebo J (2021) Valorization of khat (*Catha edulis*) waste for the production of cellulose fibers and nanocrystals. PLoS ONE 16(2): e0246794. https://doi.org/10.1371/journal.pone.0246794

Editor: Giuseppina Luciani, University of Naples Federico II, ITALY

Received: November 26, 2020

Accepted: January 26, 2021

Published: February 9, 2021

Data Availability Statement: All relevant data are within the manuscript and its Supporting Information files.

Funding: The author(s) received no specific funding for this work.

Competing interests: The authors have declared that no competing interests exist.

Abstract

Cellulose fibers (C_{40} and C_{80}) were extracted from khat (*Catha edulis*) waste (KW) with chlorine-free process using 40% formic acid/40% acetic acid (C_{40}), and 80% formic acid/80% acetic acid (C_{80}) at the pretreatment stage, followed by further delignification and bleaching stages. Cellulose nanocrystals ($CNCs_{40}$ and $CNCs_{80}$) were then isolated from C_{40} and C_{80} with sulfuric acid hydrolysis, respectively. Thus, the current study aims to isolate cellulose fibers and CNCs from KW as alternative source. The KW, cellulose fibers, and CNCs were investigated for yield, chemical composition, functionality, crystallinity, morphology, and thermal stability. CNCs were also evaluated for colloidal stability, particle size, and their influence on *in vitro* diclofenac sodium release from gel formulations preliminarily. The FTIR spectra analysis showed the removal of most hemicellulose and lignin from the cellulose fibers. The XRD results indicated that chemical pretreatments and acid hydrolysis significantly increased the crystallinity of cellulose fibers and CNCs. The cellulose fibers and CNCs exhibited Cellulose I_β crystalline lattice. TEM analysis revealed formation of needle-shaped nanoscale rods (length: 101.55–162.96 nm; aspect ratio: 12.84–22.73). The hydrodynamic size, polydispersity index, and zeta potential of the CNC_S ranged from 222.8–362.8 nm; 0.297–0.461, and -45.7 to -75.3 mV, respectively. $CNCs_{40}$ exhibited superior properties to $CNCs_{80}$ in terms of aspect ratio, and colloidal and thermal stability. Gel formulations containing high proportion of CNCs sustained diclofenac sodium release (< 50%/cm^2) over 12 h. This study suggests that cellulose fibers and nanocrystals can be successfully obtained from abundant and unexploited source, KW for value-added industrial applications.

Introduction

Khat or chat (*Catha edulis* Forsk) is an evergreen shrub native to the Horn of Africa and the Middle East. Its fresh leaves are chewed by millions worldwide as a recreational drug on daily bases for its euphoric and psychostimulant effect [1]. Ethiopia is the world's largest producer of khat which has recently become the fastest growing export commodity [2, 3]. Khat has been

used for generations by all walks of life, including children, pregnant, breastfeeding women and patients on medication [4]. Due to economic attractiveness, khat cultivation by local farmers is expanding with rapid reduction of annual crops production though the Ethiopian law on the issue of khat is in limbo neither supporting nor denouncing its use [5]. Over two million farmers produce khat on more than 250,000 ha of land [6].

When the young leaves of khat are collected for chewing locally and export, most parts of the plant such as older leaves and twigs are dumped as a solid waste. The large quantities of khat solid waste in the cities and towns have reduced the beauty of the cities/towns and became a breeding place of some rodents and vectors. Moreover, the waste encourages some people to dispose more and therefore exacerbates the poor sanitation in the cities and towns. As the waste production is so enormous, it needs proper disposal mechanism [3]. The conversion of such a waste material into useful products such as cellulose and its derivatives would alleviate a variety of socioeconomic problems, providing a greener approach to utilizing the waste through addressing the ecological and economic issues: preventing deforestation and environmental pollution, and generating foreign currency.

Recently, renewable natural resources for the development of recyclable and/or biodegradable products have received much attention to protect the environment from pollution. Lignocellulosic materials are among the most important natural sources for the production of value-added materials or biopolymers [7]. Cellulose is the most abundant polymer in nature which can be obtained from plants, animals, or bacteria. Cellulose is preferred to other polymers because of its biodegradability, abundance, light weight, cost effectiveness, high tensile strength and stiffness [8]. Cellulose and its derivatives are commonly obtained from woody plants and cotton for different industrial applications. The overuse of such sources for years by various industries such as energy and construction, has increased the need for alternative cellulose sources [9].

Nanocelluloses, also known as cellulose nanomaterials, have attracted rapidly growing scientific and technological interest from both academic and industrial researchers [10]. The two main classes of nanocelluloses are a) cellulose nanocrystals (CNCs), also referred to as nanocrystalline cellulose and cellulose nanowhiskers, and b) cellulose nanofibrils, also referred to as nano-fibrillated cellulose [11–13]. Due to higher surface area, reactive OH group in the surface, and biocompatibility among other properties, CNCs are suitable for many advanced functional applications such as tissue engineering, drug delivery, reinforcement of composite materials, etc [11, 14].

Recently, various studies have reported work of waste valorization for the production of nanocellulose from different lignocellulosic sources such as pineapple peel waste [15], *Posidonia oceanica* waste [16–18], garlic straw residues [19], industrial kelp waste [20], grass waste [21], spent coffee grounds [22], paper mill sludge [23], paper waste [24], etc.

To the best of the author's knowledge, there is no report on isolation and characterization of cellulose fibers and CNCs from an unexploited and abundant source, khat waste (KW) for potential value-added applications. The raw KW, as-extracted cellulose fibers and as-isolated CNCs were characterized with Fourier transform infrared spectroscopy (FTIR), X-ray diffraction (XRD), Scanning Electron Microscopy (SEM), Transmission Electron Microscopy (TEM), Dynamic Light Scattering (DLS), and Thermogravimetric Analysis (TGA). The CNCs were also evaluated preliminarily as a reinforcing material in carboxymethyl cellulose gel for controlled delivery of diclofenac sodium topically. CNCs offer several potential advantages in the drug delivery system. Large amounts of drugs might be bound to the surface of CNCs with the potential for high payloads and optimal control of dosing due to large surface area and negative charge [25]. Recently, CNCs-chitosan based hydrogel was fabricated for controlled delivery of theophylline, and the interaction between CNCs and chitosan is due to H-bond, van der Waals forces, and ionic and/or covalent bonds [26]. It was also reported that drugs (such as

doxorubicin hydrochloride and tetracycline hydrochloride) carrying a positive charge under physiological pH conditions, probably form strong ionic bonds with the negatively charged sulfate groups resident on the CNC surface as a result of the sulfuric acid hydrolysis process [27]. Diclofenac sodium is a non-steroidal anti-inflammatory drug widely used in the management of different inflammatory conditions, but it has short half-life around 2 h [28]. Topical/transdermal drug delivery is an attractive alternative to conventional methods because of advantages such as non-invasive delivery, constant and steady levels of drug with short biological half-life, no first-pass effect, prolonged duration of action, reduced dosing frequency, reduced drug toxicity/adverse effects, and improved patient compliance among others [29]. Thus, the aim of this study was to valorize the KW as a new and alternative source for production of cellulose and CNCs using eco-friendly method for controlled drug delivery.

Materials and methods

Materials

Khat waste was collected from Obsa Special Khat Shop, Addis Ababa, Ethiopia and cut into small pieces. Formic acid (98%) (Central Drug House (P) Ltd. New Delhi, India), acetone and sodium hydroxide 97% (HiMedia, Mumbai, India), acetic acid 99.8% (Riedel-de Haën), sulfuric acid 97% (BDH, England), copper sulfate pentahydrate 98.5%, n-hexane 99% and zinc chloride (LOBA CHEMIE-Laboratory, India), toluene (Fisher Scientific, UK), potassium iodide (Reagent chemical services Ltd Runcorn, Cheshire), ammonium oxalate 99.5% (UNI-Chem, Chemical Reagents), iodine 99%, methanol 99.9%, and ammonia solution 28% (CARLO ERBA reagents, France), ethanol absolute (Fisher Scientific, UK), hydrogen peroxide 50% (Awash Melkasa, Ethiopia), diclofenac sodium (Healthcare Limited PLC, India), triethanolamine (Fischer Chem Alert Guide, USA), potassium dihydrogen phosphate (Sörensen, Leuren, Denmark), disodium hydrogen phosphate (Fizmerk chemicals, India), sodium chloride (Oxford Laboratory, Mumbai, India), sodium carboxymethylcellulose (FMC Corporation, USA), and propylene glycol (Research-lab fine Chem. Industries, India) were used as received.

Cellulose extraction

Cellulose fibers were extracted from KW following chlorine-free conditions according to our previous method [9] with some modifications. Briefly, KW (100 g) was treated with formic acid/acetic acid (40%/40% or 80%/80% w/v) at a ratio of 70:30 of the two acids, and a waste to liquor ratio of 1:10 at the pretreatment stage on a water bath at 90˚C for 1.5 h. After repeated washing and filtration, the pulps were then treated with 2.5% NaOH for 1 h, followed with a mixture of 20% formic acid/20% acetic acid/7.5% hydrogen peroxide (2:1:2) solution on a water bath at 90˚C for 1.5 h, at a waste to liquor ratio of 1:10 with continuous washing with hot water. Lastly, bleaching was performed using 10% hydrogen peroxide in alkaline media (adding 40 g of sodium hydroxide) at 1:10 fiber ratio, first at room temperature, followed by heating on water bath at 70˚C, for 30 min each. The pulps were then washed continually with hot distilled water, and finally dried in an oven (Kottermann® 2711, Germany) for 1 day at 60˚C. The as-obtained cellulose fibers were named as C_{40} and C_{80}, respectively.

Isolation of CNCs

CNCs were isolated from KW following the method described elsewhere with few modifications [7, 30–33]. The cellulose fibers (C_{40} and C_{80}) extracted from KW were first hydrolyzed with 64% (w/w) sulfuric acid (1:20 g/mL) at 45˚C for 60 min under magnetic stirrer (the resulting NCs designated as $CNCs_{40}$ and $CNCs_{80}$). The mixture was then diluted 10-fold with ice

cubes to stop the reaction, and washed by successive centrifugations at 4˚C (Beckman Coulter Allegra 64R Refrigerated Centrifuge, USA) for 10 min each at 10,000 rpm. The mixture was also dialyzed against distilled water using dialysis sacks (Avg. flat width 35 mm, MWCO 12,000 Da, Sigma-Aldrich, USA) until neutral pH was reached (5 days). Subsequently, the resulting suspension was homogenized using a disperser type UltraTurrax (Janke and Kunkel IKA-Labortechnik, Ultra-Turrax T50) for 5 min at 10,000 rpm twice and sonicated (Sonics and Materials Inc. Vibracell, VCX 750, Newtown CT, USA) in an ice bath for 5 min. The aqueous suspension was freeze-dried in a lyophilizer (Operon Co., Ltd.—Bio-Equip, Korea) and dried for 72 h to obtain CNCs powder. The yields of CNCs were estimated gravimetrically considering the initial weight of the extracted cellulose fibers (C_{40} and C_{80}).

Composition of the untreated KW and cellulose, and identification tests

The constituents of the untreated KW as well as as-obtained cellulose fibers such as lignin, hemicellulose and others were determined according to the methods stated elsewhere [9, 34–37], as described in the S1 Appendix. Solubility, appearance, color test, pH, ash values and moisture content of the as-obtained cellulose fibers from KW were determined according to the methods described in pharmacopeia [38].

Characterization of the materials

Fourier-transform infrared (FTIR) spectroscopy. FTIR tests were performed on a Perkin Elmer FTIR spectrometer (L1600400 Spectrum TWO DTGS, SN: 108152, LIantrisant, UK) in the infrared range from 4000 to 450 cm^{-1}, with no further sample preparation.

X-ray diffraction (XRD). XRD was performed to investigate the crystallinity of as-isolated CNCs and cellulose precursors using an XRD-7000 X-ray Diffractometer MAXima (SHIMADZU Corporation, Japan) at 40 kV, 30 mA with monochromatic Cu-Kα radiation. XRD data were collected over an angular range of 10 to 40˚ in a sampling pitch of 0.0200˚ and scan speed of 3.0000˚/min at room temperature.

The crystalline index (CrI) was determined using the equation proposed by Segal et al. (1959) (Empirical method):

$$CrI = \frac{(I_{200} - I_{am})}{I_{200}} x100\%$$

Where, I_{200} is the maximum intensity (in arbitrary units) of the diffraction from the 200 plane, and I_{am} is the intensity of the background scatter.

X-ray diffraction of the cellulose fibers and as-isolated CNCs were deconvoluted following Gaussian profile, and parameters such as d-spacings (d), apparent crystallite size or thickness for the 200 plane (τ_{200}), fractional variation in the plane spacing for the 200 plane $(\Delta d/d)_{200}$, the proportion of crystallite interior chains for the 200 plane (X_{200}), and Z-values were determined using equations described elsewhere [8, 9, 39, 40], and provided in the S2 Appendix.

Environmental Scanning Electron Microscopy (ESEM). ESEM observations were evaluated using ESEM FEI/Philips XL-30 ESEM (Leuven, Belgium) at accelerating voltage of 2.00 KV. The samples were coated with chromium using vacuum sputter prior to SEM analysis.

Transmission Electron Microscopy (TEM). Droplets of CNCs suspension (0.05% w/v) were deposited on a formvar-coated copper grid. The specimen was negatively stained with a 1% (w/v) phosphotungstic acid solution and dried at room temperature. The TEM observations were conducted using an EM 900 TEM (Carl Zeiss Microscopy, Jena, Germany; acceleration voltage 80 kV), and the micrographs were taken with a slow scan camera (Variospeed SSCCD camera SM-1k-120, TRS, Moorenweis, Germany).

Particle size analysis. Particle size and PDI analysis of the CNCs were determined by photon correlation spectroscopy (PCS) using a 90Plus Particle Size Analyzer 28 (Brookhaven Instruments Corporation, New York, USA). Prior to the measurements, the CNCs suspensions were diluted using distilled water to yield an appropriate scattering intensity. All experiments were done at least in triplicate at 25˚C.

Zeta Potential (ZP). The ZP of aqueous suspension of CNCs (0.05% w/v) in 0.1N PBS was measured using Malvern Instruments Zetasizer Nano ZS working on electrophoretic mobility at 25˚C after 120 s equilibration time and a wavelength of 659 nm.

Thermal analysis. The thermogravimetric analysis (TGA) and its derivative (DTG) of the as-obtained CNCs and cellulose precursors were studied TGA/DTG-60H (SHIMADZU Corporation, Japan). The samples were heated from room temperature to 700˚C at a heating rate of 10˚C/min under a nitrogen gas flow rate of 60 mL/min.

Preparation of diclofenac sodium gel formulations

CNCs colloidal dispersions (0.25 to 2%) and CMC at a concentration of 2% (w/w) were prepared as gelling agent. Five of the medicated formulations (F1-F5) were prepared varying the concentrations of CNCs according to the formulae given in Table 1, and the other formulation containing no CNC. The medicated hydroalcoholic gel formulations were prepared by dissolving diclofenac sodium and sodium benzoate (SB) in a co-solvent of ethanol and propylene glycol (PG). Subsequently, the solution containing the drug was added to the gelling agent prepared in a known portion of distilled water under continuous stirring to yield a homogenous dispersion, which was in turn neutralized with triethanolamine to obtain a colorless gel. The final weight of the formulations was finally adjusted with distilled water [41–43].

UV calibration curve of diclofenac sodium

Eight different concentrations (2, 4, 6, 8, 10, 12, 14, and 16 μg/ml) were prepared from stock solution containing 100 μg/ml of diclofenac sodium in PBS (pH 7.4). The UV absorbance readings of these solutions were measured at 276 nm using UV/Visible spectrophotometer (PG Instruments Limited, T92+, Leicestershire, UK). PBS (pH 7.4) was used as a blank. The absorbance versus concentration of solutions was plotted and a calibration curve with a linear regression equation of: $Y = 0.0454X + 0.0512$ (where, Y is the absorbance and X is the concentration in μg/ml) and correlation coefficient of 0.9987 was obtained (Fig 1).

Physicochemical evaluation of diclofenac sodium gel formulations

The prepared diclofenac sodium gel formulations were evaluated for clarity/transparency, color, scent, texture, consistency, homogeneity, drug content, rheology, clarity, spreadability, extrudability, pH, and kinetics and mechanism of drug release [41, 43–45]. The detailed procedure is put in the S3 Appendix.

Table 1. Composition % (w/w) of different diclofenac sodium gel formulations.

Formulation	Diclofenac sodium (g)	CMC (g)	CNCs (g)	Ethanol (g)	PG (g)	Triethanolamine (g)	SB (g)	Distilled water qs (g)
F0	3	2	0	10	10	3	0.135	100
F1	3	2	0.25	10	10	3	0.135	100
F2	3	2	0.5	10	10	3	0.135	100
F3	3	2	0.75	10	10	3	0.135	100
F4	3	2	1	10	10	3	0.135	100
F5	3	2	2	10	10	3	0.135	100

https://doi.org/10.1371/journal.pone.0246794.t001

In vitro release study of diclofenac sodium from gel preparations

One-gram gel formulation each containing 30 mg of diclofenac sodium was placed on cellulose acetate membrane (pore size 0.45 μm, Sartorius, Goettingen, Germany) and fixed to one end and made water-tight with aid of a rubber band in an apparatus consisting of cylindrical tube with both ends open, with 12.1 mm inner diameter (release area = 115 mm^2) as a diffusion cell. The tubes were submerged in 1000-ml vessels containing 400 ml PBS (pH 7.4) as receptor medium. The whole assembly was fixed in such a way that the lower end of the cell containing the gel just touched (1–2 mm deep) the diffusion medium. The release test was carried out at a controlled stirring rate of 100 rpm to ensure sink condition and a temperature of 37 ± 1˚C by means of water jacket surrounding each cell, based on the facts that the receptor phase is in contact with the deepest skin layers and that the deep body temperature of humans is maintained between 36.2˚C and 37.2˚C in order to maintain the skin surface at 32˚C. An aliquot of 5 mL was withdrawn at specific time intervals up to 720 min, and estimated spectrophotometrically at 276 nm. After each withdrawal, the diffusion medium was replaced with an equal volume of fresh diffusion medium. The cumulative percent release was calculated for each time (in min) interval [41, 43, 45].

Statistical analysis

All data were analyzed using OriginPro 8.5.1 (OriginLab Corporation, MA, USA) and Excel 2016. The experiments were done in triplicates and the data were presented as the mean ± standard deviation (SD). All data reported in this study were the averages of triplicate determinations. *P* value of less than 0.05 was considered to be evidence for a significant difference, and a Tukey's test for one-way analysis of variance (ANOVA) was applied when necessary.

Results and discussion

Cellulose extraction conditions

In this study, cellulose fibers were extracted with two conditions using 40% formic acid/40% acetic acid, and 80% formic acid/80% acetic acid at the pretreatment stage. It was reported that acetic acid and formic acid can effectively remove lignin and hemicelluloses by cleaving ether bonds between lignin and hemicellulose from different lignocellulosic materials at atmospheric pressure [46, 47].

Hydrogen peroxide in formic acid/acetic acid solution enhanced the delignification process due to the combined effect of the organic acids as solvent and peroxyacid as an oxidizing agent to dissolve the lignin by the action of hydroxonium ion OH^+ [9, 48]. Bleaching the mass with a solution of hydrogen peroxide in an alkali medium, a chlorine-free bleaching agent, is carried out for the elimination of chromophore compounds to raise the brightness of cellulose, reduce chlorinated organic matter and the effluent odor, which is an important characteristic to produce cellulose derivatives.

Furthermore, a chlorine-free bleaching technique was followed, where oxidation of lignin through cleavage of side chains occurs due to the formation of the perhydroxyl anion (OOH-), a nucleophile intermediate. The action of radicals formed during the bleaching process is responsible to a large extent for the delignification. The bleaching with peroxide causes degradation of the molecule into smaller and water soluble parts [48]. Basically, the chromophore compounds constitute fragments of lignin. Therefore, it is expected that in this process mainly lignin is removed most, preserving the polysaccharides [49].

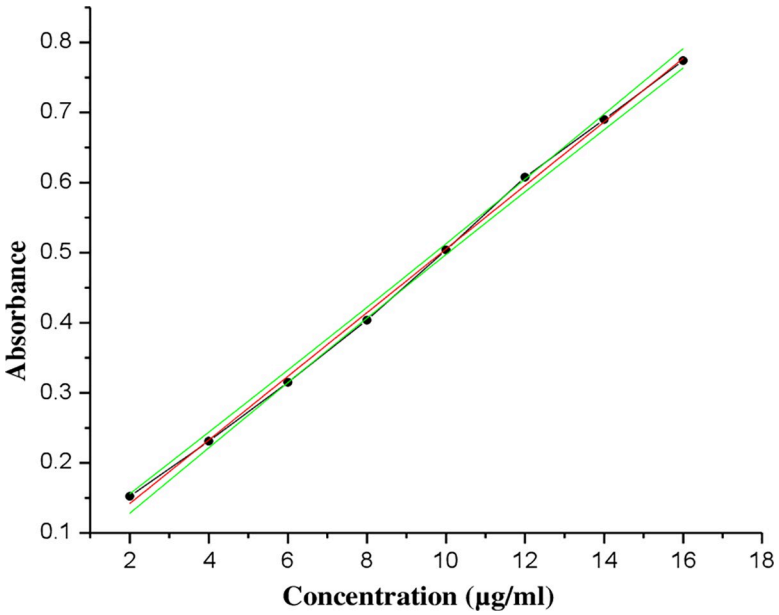

Fig 1. The UV absorption calibration curve of diclofenac sodium in PBS (pH 7.4) at 276 nm with 95% confidence bands for mean, (r^2 = 0.9987).

https://doi.org/10.1371/journal.pone.0246794.g001

Identification and composition of the plant materials

The cellulose fibers extracted from KW were white, and fluffy and fibrous in nature, and soluble in cuprammonium hydroxide 'Cuam' solution, but insoluble in water, acetone, anhydrous ethanol and toluene. A violet-blue color was formed when the extracted cellulose fibers were dispersed in iodinated zinc chloride solution, fulfilling the parameters specified in pharmacopeia [50]. The macroscopic images of the untreated KW, and as-extracted cellulose fibers (C_{40} and C_{80}) are shown in Fig 2.

The composition of untreated KW and as-obtained cellulose fibers such as cellulose content, hemicellulose, and lignin is presented in Table 2. Cellulose content increased in the extracted cellulose fibers due to removal of non-cellulosic components [9, 49]. Other studies also reported the increment of cellulose content after chemical treatments of the raw

Fig 2. Photographs of untreated khat waste (KW-0), and as-extracted cellulose fibers (C_{40} and C_{80}) from left to right.

https://doi.org/10.1371/journal.pone.0246794.g002

Table 2. Chemical composition of untreated KW, and as-obtained cellulose fibers, and other sources.

Plant materials (References)		Composition (%w/w) on dry basis							
		Cellulose	Hemicellulose	Klason lignin	Pectic matters	Fatty and waxy matters	Aqueous extractives	Ash	Others
KW*	0	39.4 ± 0.38	12.75 ± 0.52	28.67 ± 2.46	5.24 ± 0.66	7.87 ± 0.18	3.47 ± 0.35	3.40 ± 0.12	---
	C_{40}	82.7 ± 1.43	5.83 ± 0.52	10.89 ± 0.21	0.98 ± 0.07	0.73 ± 0.06	0.66 ± 0.13	1.34 ± 0.18	---
	C_{80}	88.4 ± 1.43	3.44 ± 0.48	6.93 ± 0.18	0.88 ± 0.06	0.67 ± 0.11	0.64 ± 0.04	0.97 ± 0.09	---
Banana pseudo-stem [54]		23.82	25.69	8.56	5.03	4.25	32.64	7.06	---
Corn husk [35]		45.13 (α)	31.15 ± 0.55	14.32 ± 0.23	3.65 ± 0.17	2.20 ± 0.11	2.50 ± 0.07	---	1.05
Coffee silverskin [51]	0	31 ± 2%	---	---	---	---	---	2.7 ± 0.8	---
	C	73.60–85.50	---	---	---	---	---		---
Sugarcane bagasse [52]	0	42.10	26.10	24.40	---	---	---	1.3	6.1
	C	93.20	3.40	2.30	---	---	---	0.45	0.65
Sugarcane bagasse [34]		40.21	25.00	23.90	---	---	---	1.72	---
Garlic straw residues [19]	0	41	18	6.3		3.2		10	
	C	86	---	---	---	---	---	9.4	---

*Current study, 0-Raw materials; C-Extracted cellulose; Data were presented as the mean ± SD (n = 3).

https://doi.org/10.1371/journal.pone.0246794.t002

lignocellulosic materials such as coffee silverskin [51] and sugarcane bagasse [52] (Table 2). The brightness, digestibility, and weight of KW cellulose fibers were considerably improved when 80% formic acid and 80% acetic acid (70:30) were used instead of 5% or 10% wt sodium hydroxide at the pretreatment stage. It has been reported that alkaline treatment is very effective in increasing the digestibility of hardwood and agricultural residues with low lignin content [53]. The cellulose content in the untreated khat waste (39%) was comparable with sugarcane bagasse (40–42%) [34, 52], and garlic straw residues (41%) [19], but higher than banana pseudo-stem (24%) [54] and coffee silverskin (31%) [51], and lower than corn husk (45%) [35] (Table 2).

Reduction of non-cellulosic materials is observed in the as-extracted cellulose, and increase in the cellulose content, which is in agreement with studies reported elsewhere [19, 49, 55]. The CNCs suspensions were white and turbid in appearance. The yields of $CNCs_{40}$ and $CNCs_{80}$ obtained from C_{40} and C_{80} were 55% and 49%, respectively.

As the lignin content (29%) reported in this study (Table 2) is much higher than that reported in most studies: 14% (sisal fibers) [56], 9% (municipal grass waste) [21], and 9% (lemon seeds) [57], the use of acetic acid and formic acid in the pretreatment step was needed to increase the purity of cellulose and facilitate the removal of lignin as well as digestibility, and thereby enhance the whiteness of the pulps. However, in a preliminary work during extraction of cellulose from other lignocellulosic materials with low lignin content, the whiteness, cellulose content as well as the degree of crystallinity increased significantly without such additional step. Different studies which employ sodium hydroxide in the pretreatment stage use chlorine containing bleaching agents mainly sodium chlorite solution [21, 57–60] during isolation of CNCs, however, a chlorine-free bleaching solvent (alkaline hydrogen peroxide) was employed in our study.

Chemical functionality studies

Fig 3 illustrates the FTIR spectra of untreated KW, as-obtained cellulose fibers, and CNCs. FTIR spectroscopy revealed the similarities of all spectra of cellulose fibers and CNCs, showing similar chemical composition among the samples [61]. The broad absorption band around 3340 cm^{-1} is due to the stretching vibrations of the OH groups, indicating the hydrophilic

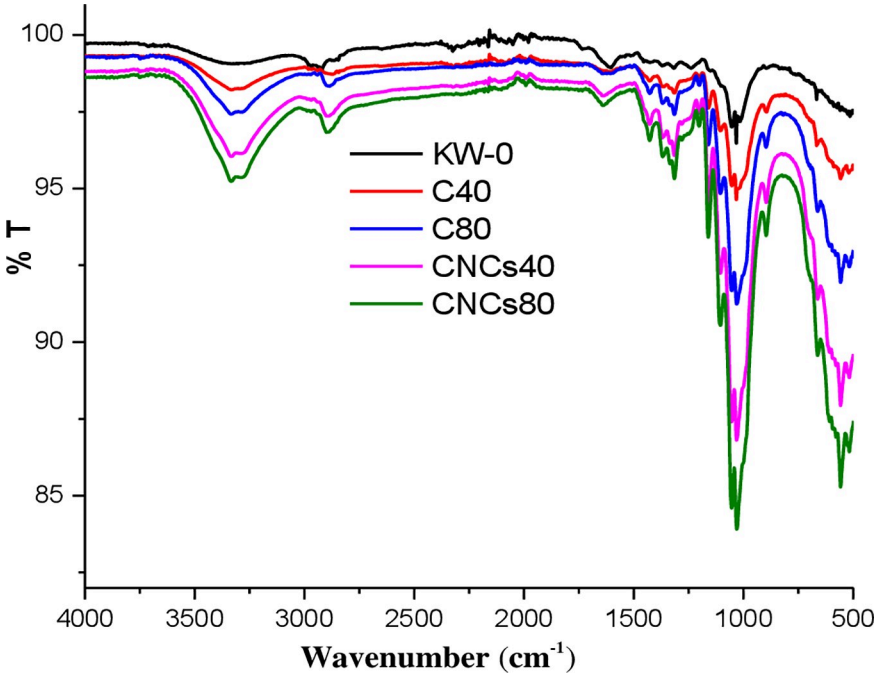

Fig 3. FTIR spectra of untreated KW, as-obtained cellulose fibers (C_{40} and C_{80}) and CNCs ($CNCs_{40}$ and $CNCs_{80}$). (Key: KW-0: untreated khat waste; C_{40} and C_{80}: cellulose fibers obtained from khat waste with 40% formic acid and 40% acetic acid, and 80% formic acid and 80% acetic acid, respectively at the pretreatment stage; $CNCs_{40}$ and $CNCs_{80}$: cellulose nanocrystals isolated from C_{40} and C_{80}, respectively).

https://doi.org/10.1371/journal.pone.0246794.g003

tendency of the materials. The weak band around 2900 cm^{-1} is due to the asymmetric stretching vibration of the CH_2 bond [62]. Furthermore, the appearance of a peak at ~1645 cm^{-1} in all the spectra shows absorption of water by the materials [40].

The untreated KW indicated typical peaks around 1736 cm^{-1}, 1516 cm^{-1}, and 1235 cm^{-1}. The disappearance of the peak around 1736 cm^{-1} showed the cleavage of the linkages between ferulic acid or p-coumaric acid or (p-) hydroxycinnamic acids and lignin during chemical treatment. The absence of the bands around 1516 cm^{-1} and 1235 cm^{-1} in the cellulose fibers and CNCs indicated that lignin functional groups such as aromatic rings were dissociated and dissolved. Similar findings were also reported by different research groups indicating removal of non-cellulosic materials using different treatment conditions [9, 51, 63, 64].

The absorption band at around 1428 cm^{-1} is associated with intermolecular hydrogenattraction at the C_6 group. The peak around 1323 cm^{-1} region of the spectra is attributed to the bending vibration of the CH and CO groups of aromatic ring in the materials [61]. The peak around 896 cm^{-1} is due to C_1H rocking vibration of cellulose (β-glycosidic linkages). The bands around 3340, 2900, 1428, 1323, and 896 cm^{-1} in all cellulose and CNCs spectra are associated with the characteristics of cellulose I, showing that the acid hydrolysis did not affect the chemical structure of the cellulosic fragments [65, 66].

Crystallinity analysis

The as-isolated $CNCs_{40}$ and $CNCs_{80}$ like their cellulose precursors and untreated KW (KW-0) displayed a typical crystal lattice of Cellulose I, with the main diffraction signals around 2θ values of 15˚, 16˚, 22˚ and 34˚ with assigned crystallographic plane of 1-10, 110, 200 and 040, respectively after deconvolution using Gaussian profile as reported elsewhere [61, 64, 67]. The XRD patterns of the untreated KW, as-obtained cellulose and CNCs are shown in Fig 4.

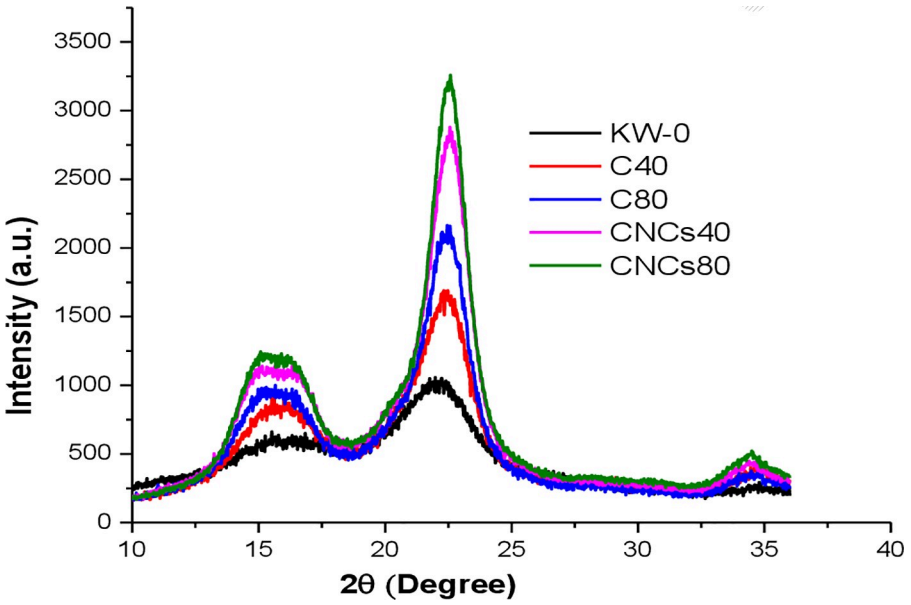

Fig 4. XRD of untreated KW, as-obtained cellulose fibers (C_{40} and C_{80}) and CNCs ($CNCs_{40}$ and $CNCs_{80}$). (Key: KW-0: untreated khat waste; C_{40} and C_{80}: cellulose fibers obtained from khat waste with 40% formic acid and 40% acetic acid, and 80% formic acid and 80% acetic acid, respectively at the pretreatment stage; $CNCs_{40}$ and $CNCs_{80}$: cellulose nanocrystals isolated from C_{40} and C_{80}, respectively).

https://doi.org/10.1371/journal.pone.0246794.g004

$CNCs_{80}$ (82.84%) exhibited almost comparable CrI with $CNCs_{40}$ (81.60%), but much higher than that of untreated KW (56.89%). Removal of non-cellulosic was also confirmed by the increment of CrI of cellulose fibers when compared to the untreated KW (Fig 4 and S1 Table). Generally, the CrIs increased in both isolated CNCs when compared to their cellulose precursors. Such an increment of crystallinity was due to the removal of hemicellulose and lignin existing in amorphous regions, and during the hydrolysis process [68]. The CrIs of CNCs reported in this study were higher when compared to CrIs of CNCs isolated from others sources such as passion fruit peels waste (77.96%) [14], pineapple crown waste (73%) [69], seaweed (60%) [68], and pueraria root residue (60%) [70].

The τ values of the $CNCs_{40}$ and $CNCs_{80}$ were 5.466 nm and 5.633 nm, and X values were 0.630 and 0.672, respectively. S1 Table shows different parameters obtained from the (deconvoluted) XRD of untreated KW, as-extracted cellulose, and $CNCs_{40}$ and $CNCs_{80}$. The d-spacings of the all the samples ranged from 0.589-0.608, 0.523-0.565, 0.385-0.401, and 0.258-0.262 for the planes of 1-10, 110, 200, and 040, respectively as shown in S1 Table. All the samples including $CNCs_{40}$ and $CNCs_{80}$ are all I_{β}-type cellulose, as confirmed by XRD patterns, d-spacing values, and the negative numbers of the Z-Values [71, 72] (S1 Table).

Morphological, dimensional and zeta potential investigation

Pretreatment using formic acid and acetic acid, followed with delignification/bleaching stages resulted in changes of chemical composition of the as-obtained cellulose fibers and the structure of the fibers surfaces. The surface morphology of untreated KW and as-extracted cellulose is investigated with SEM as shown in Fig 5. SEM images indicated that untreated KW existed as rough and compact fibrillar packing displaying lot of non-cellulosic components such as lignin scattered over the cellulosic fiber surface, acting as cementing materials, consistent with other finding [73]. The cellulose bundles are composed of individual fibers linked together by the massive cementing material. Most of the lignin and hemicellulose were hydrolyzed during

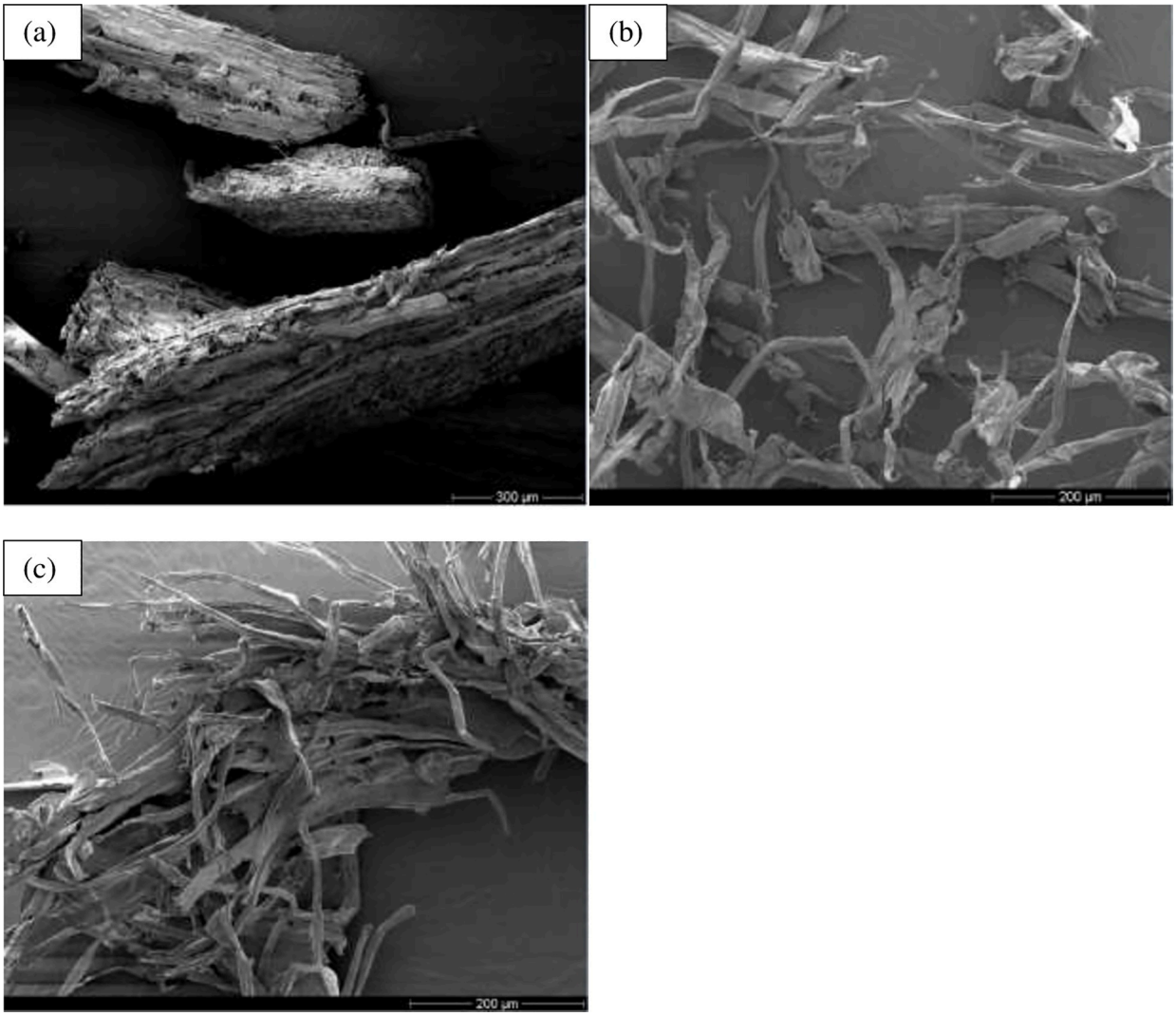

Fig 5. Scanning electron micrographs of (a) untreated khat waste (KW-0, with scale bar of 300 μm), and as-obtained cellulose fibers: (b) $C_{40,}$ and (c) C_{80} (with scale bar of 200 μm).

https://doi.org/10.1371/journal.pone.0246794.g005

chemical treatments. The average diameters of the as-extracted cellulose fibers (16 and 28 μm) are much smaller than that of untreated KW (263 μm) (Table 3), indicating the removal of non-cellulosic components during the treatment conditions. In a study reported elsewhere, the diameter of untreated sisal fibers ranged from 100–500 μm and the diameter of the extracted cellulose fiber was reduced to 7–31 μm [74].

TEM images show appearance of needle-shaped CNCs on the acid hydrolysis and sonication with a scale bar of 200 nm (Fig 6). From the TEM analysis, the length and diameter of the CNCs isolated from the byproducts ranged from 106.78-193.06 nm and 5.16-11.79 nm, respectively. Furthermore, the average aspect ratio of the CNCs ranged from 17.32-36.68 (Table 3).

The DLS results also supported the TEM results that the isolated CNCs were in nanoscale range, and their hydrodynamic size were 362.8 nm and 222.8 nm for $CNCs_{40}$ and $CNCs_{80}$, respectively (Table 3). The DLS and TEM results suggested that increasing the concentration of weak acids at the pretreatment stage contributed for reduced particle size and aspect ratios of the isolated CNCs. The ZP of the CNCs suspensions ranged from -45.7 and -75.3 mV in

Table 3. Average diameters (SEM) of the untreated KW, and as-extracted cellulose fibers (C_{40} and C_{80}), and TEM dimensional analysis, DLS and Zeta potential values of the CNCs.

CNCs	Length (L) range; $L_{average}$ (nm)	Diameter (D) range; $D_{average}$	Aspect ratio	Hydrodynamic size (nm); PDI (from DLS)	ZP (mV)
KW-0	--	263.04 ± 45.37 μm	--	--	--
C_{40}	--	27.97 ± 12.20 μm	--	--	--
C_{80}	--	16.08 ± 3.02 μm	--	--	--
$CNCs_{40}$	162.96 ± 26.04	7.17 ± 1.86 nm	22.73	362.8; 0.461	-75.3
$CNCs_{80}$	101.55 ± 20.53	7.91 ± 2.56 nm	12.84	222.8; 0.297	-45.7

(Key:- KW-0: untreated khat waste; C_{40} and C_{80}: cellulose fibers obtained from khat waste with 40% formic acid and 40% acetic acid, and 80% formic acid and 80% acetic acid, respectively at the pretreatment stage; $CNCs_{40}$ and $CNCs_{80}$: cellulose nanocrystals isolated from C_{40} and C_{80}, respectively; $D_{average}$-average diameter of untreated KW, cellulose fibers, and CNCs estimated using ImageJ Software; $L_{average}$-average length of CNCs; PDI: Polydispersity index; ZP: Zeta potential). Data were presented as the mean ± SD ($n > 15$).

https://doi.org/10.1371/journal.pone.0246794.t003

neutral water and 0.1 N PBS (S1 Fig and Table 3), and resulted in stable colloidal suspensions as the absolute values obtained are higher than -15 mV which is the minimum value to represent the onset of agglomeration [33, 75, 76]. ZP of CNCs at the values near or lower than -20 mV at low concentrations remain stable [77].

Thermal properties

Fig 7 demonstrates the thermogravimetric (TG) and derivative thermogravimetric (DTG) curves of the untreated KW, as-extracted cellulose fibers and CNCs. The thermal degradation data (ΔT), ($T_{10\%}$), ($T_{50\%}$), weight loss (rate) at each region (%), the residual weight at 500 and 700˚C as well as the peak degradation temperatures (T_{max}) are listed in S2 Table. The small weight loss (3.85-6.38%) in the region 30-120˚C is mainly due to loss of water adsorbed to the materials [12, 15, 60, 70, 78]. The as-obtained cellulose fibers and CNCs contained relatively lower moisture than respective untreated KW as shown in S2 Table, which might be due to the removal of hydrophilic components such as hemicellulose and lignin in cellulose fibers and CNCs [73].

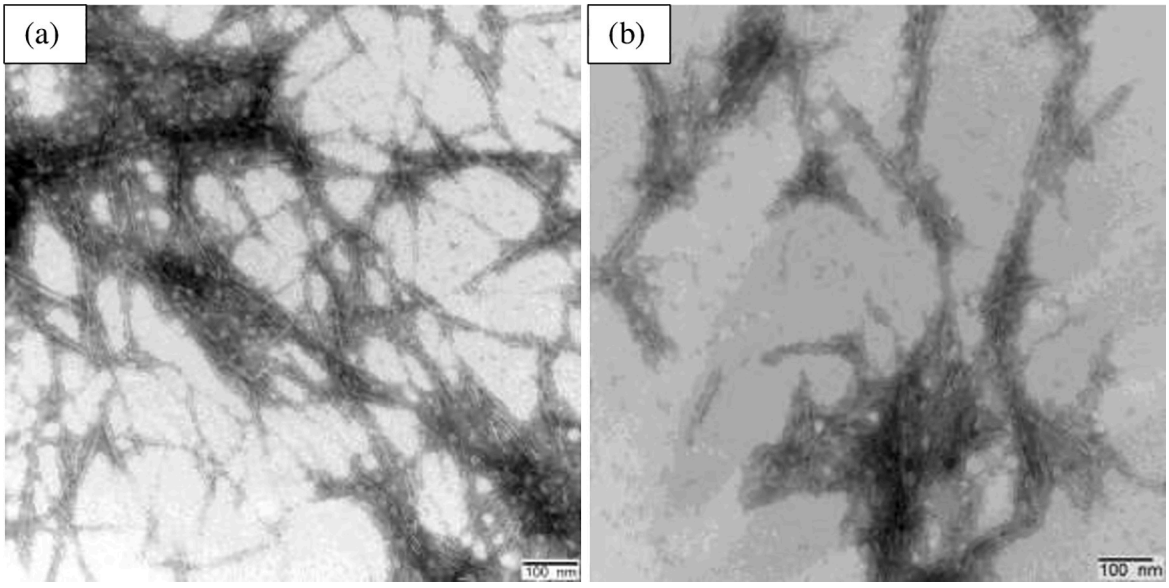

Fig 6. Transmission electron micrographs of CNCs isolated from KW: $CNCs_{40}$ (a) and $CNCs_{80}$ (b) (Bar scale: 100 nm).

https://doi.org/10.1371/journal.pone.0246794.g006

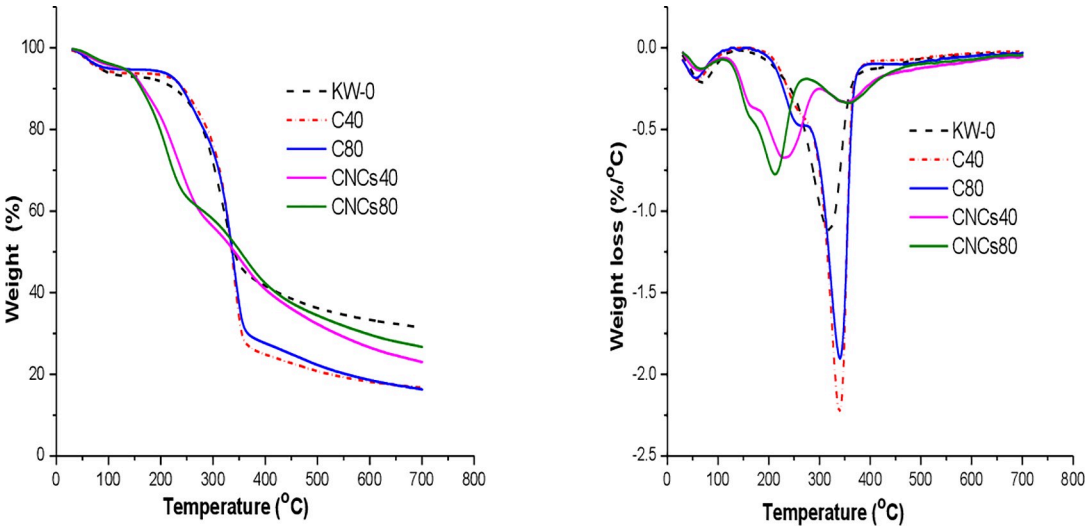

Fig 7. Thermal degradation behaviors: TGA (a) and DTG (b) of untreated KW (KW-0), as-obtained cellulose fibers (C_{40} and C_{80}) and CNCs ($CNCs_{40}$ and $CNCs_{80}$). (Key:- KW-0: untreated khat waste; C_{40} and C_{80}: cellulose fibers obtained from khat waste with 40% formic acid and 40% acetic acid, and 80% formic acid and 80% acetic acid, respectively at the pretreatment stage; $CNCs_{40}$ and $CNCs_{80}$: cellulose nanocrystals isolated from C_{40} and C_{80}, respectively).

https://doi.org/10.1371/journal.pone.0246794.g007

The DTG thermograms of untreated KW and as-extracted cellulose fibers showed a sudden reduction in weight loss around 189 °C, mainly due to the loss of hemicellulose. The acetyl groups of hemicellulose contributed for the low thermal stability. A major weight loss was observed at T_{max} 320–400 °C due to depolymerisation, dehydration and decomposition of the glycosidic units of cellulose [33]. There was poor/no identifiable peak of lignin in the TGA/DTG thermograms of the samples including untreated KW due to its slow and resistant decomposition ranging from ambient temperature to 700 °C [65].

The CNCs exhibited a weight loss of 34-38% in the region at T_{max} 213 and 232˚C due to degradation of surface sulfate groups lowering the activation energy and large specific surface area, when compared to the cellulose precursors (weight loss of 67-69% at T_{max} of 340˚C. Another decomposition step with a weight loss of 22% exhibited at T_{max} ranging from ~360˚C (the major cellulose degradation temperature), due to breakdown of the interior non-sulfated cellulose crystals [60]. The CNCs also exhibited lower maximum weight loss rates (0.6726-0.7744%/˚C) in the sulfated cellulose groups than the cellulose counterparts (1.9019–2.2346%/˚C). The char residues at 550˚C and 700˚C of the isolated CNCs showed higher values than cellulose counterparts because of a dehydration effect of the sulfate group as flame retardants [20, 60, 78, 79].

Evaluation of diclofenac sodium gel formulations

Five different topical diclofenac sodium gel formulations containing CNCs were prepared as a reinforcing material in CMC gel base, however, the sixth one did not contain $CNCs_{40}$. $CNCs_{40}$ was selected as it had better aspect ratio and colloidal stability when compared to $CNCs_{80}$. All diclofenac sodium gel formulations were smoothly spreadable without any solid or gritty particles, homogeneous, and transparent in physical appearance. The presence of triethanolamine in the medicated gel formulations improved the clarity when compared with the polymer gel bases, suggesting the solubility of the drug in the gel matrix. Triethanolamine was incorporated to adjust the pH and to increase the solubility of the drug in the gel formulations [45, 80].

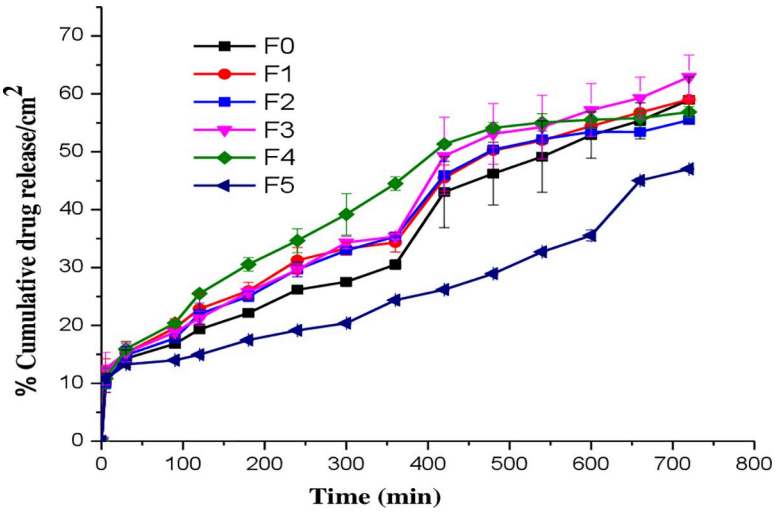

Fig 8. ***In vitro*** **diclofenac sodium release profiles from gel formulations (F0-F5).**

https://doi.org/10.1371/journal.pone.0246794.g008

The pH values of diclofenac sodium gel formulations varied from 6.81 ± 0.042–7.43 ± 0.033, which is physiologically acceptable pH range and free from any skin irritation. The content uniformity of diclofenac sodium in all gel formulations ranged from 98.76 ± 0.41–101.2 ± 0.52% which are within the acceptable limits [50]. In the spreadability test, the diameters of diclofenac sodium gel formulations ranged from 54 ± 3.4–72 ± 2.5 mm. Viscosity is an important physical parameter for characterizing the gel formulations as it affects the extrudability, spreadability, and release of drug and other physicochemical properties of gel preparations. The viscosity of the gel formulations declined proving shear-thinning flow when the shear rate varied from 0.5 to 200 rpm (67 to 6667 sec^{-1}) (S2 Fig).

In vitro release and kinetics of diclofenac sodium

From the release profiles of diclofenac sodium from the six gel formulations as depicted in Fig 8, it is observed that, initially (~1 h), the drug was released rapidly (burst effect) followed by a slow release for the rest of the 12 h study period. The initial burst effect could be due to the release of the drug to the surface of the immediate barrier membrane. The results show that when the concentration of CNCs in the gel formulations increased from 0.25 to 2% (w/w), the percent of diclofenac sodium released into the buffered medium gradually decreased to 47%/cm^2.

The drug release pattern best followed Higuchi kinetic models when the data were analyzed and compared with zero order, and first order kinetics, as confirmed by the good correlation coefficients (S3 Table). This finding indicates that the rate-controlling stage in the release process is the diffusion of the dissolved drug through the vehicle network to the external medium. As the viscosity of gels increase, the release the drug becomes slower by extending dissolution time and prolonging drug diffusion through the gel matrix. The viscosity of vehicles may play an important role in controlling the drug release when the drug diffusion through the vehicle is a rate limiting step.

Conclusions

The present research includes successful extraction of cellulose fibers and CNCs from abundantly available KW using two chlorine-free isolation conditions. Removal of non-cellulosic

materials such as hemicellulose and lignin were confirmed by the FTIR, XRD and SEM studies. The untreated KW, as-obtained cellulose fibers, and CNCs exhibited the typical peaks of Cellulose I_β around 15, 16, 22 and 34˚ 2θ, as confirmed by XRD pattern, d-spacings, and Z-values. The increment of formic acid/acetic acid concentration from 40% to 80% did not significantly increase CrI of the CNCs after acid hydrolysis. Additionally, higher/comparable yield, aspect ratio, colloidal and thermal stability were observed in $CNCs_{40}$. The CNCs can be used as a reinforcing material to increase the gel strength, and enhance sustained delivery of drugs. The findings suggest that cellulose fibers and CNCs can be obtained from KW as alternative source using ecofriendly method.

Supporting information

S1 Appendix. Methods for determination of the composition of the plant materials.
(DOCX)

S2 Appendix. Physicochemical evaluation of the medicated gel formulations.
(DOCX)

S3 Appendix. Equations for the determination of different parameters from (deconvoluted) XRD diffractograms.
(DOCX)

S1 Fig. Zeta potential of a) CNCs40 and b) CNCs80.
(DOCX)

S2 Fig. Rheological profiles of diclofenac sodium gel formulations (F0-F5).
(DOCX)

S1 Table. Properties obtained from the (deconvoluted) XRD of untreated KW, as-obtained cellulose fibers, and CNCs.
(DOCX)

S2 Table. Summary of thermal properties of untreated khat waste, obtained cellulose, and CNCs.
(DOCX)

S3 Table. *In vitro* diclofenac sodium release characteristics from the gel formulations and fitting models.
(DOCX)

Acknowledgments

The authors acknowledge Adama Science and Technology University, Ethiopian Pharmaceutical Manufacturing Sh.Co., and Cadila Pharmaceuticals, Ethiopia for providing us access to different instruments and materials.

Author Contributions

Data curation: Jemal Dilebo.

Investigation: Kebede Wondu.

Methodology: Tesfaye Gabriel, Kebede Wondu.

Project administration: Jemal Dilebo.

Resources: Tesfaye Gabriel, Kebede Wondu, Jemal Dilebo.

Software: Tesfaye Gabriel.

Supervision: Tesfaye Gabriel.

Validation: Tesfaye Gabriel, Kebede Wondu, Jemal Dilebo.

Visualization: Kebede Wondu.

Writing – original draft: Tesfaye Gabriel.

Writing – review & editing: Kebede Wondu, Jemal Dilebo.

References

1. Nichols T, Khondkar P, Gibbons S. The psychostimulant drug khat (Catha edulis): A mini-review. Phytochem Lett. 2015; 13: 127–133. https://doi.org/10.1016/j.phytol.2015.05.016
2. Kandari LS, Yadav HR, Thakur AK, Kandari T. Chat (Catha edulis): a socio economic crop in Harar Region, Eastern Ethiopia. J Korean Phys Soc. 2014; 3: 1–9. https://doi.org/10.1186/2193-1801-3-579 PMID: 25332879
3. Rameshwar HY, Argaw A. Manurial value of khat waste vermicompost from Awday, Harar town, Ethiopia. Int J Recycl Org Waste Agric. 2016; 5: 105–111. https://doi.org/10.1007/s40093-016-0121-y
4. Bedada W, de Andrés F, Engidawork E, Hussein J, LLerena A, Aklillu E. Effects of Khat (Catha edulis) use on catalytic activities of major drug-metabolizing cytochrome P450 enzymes and implication of pharmacogenetic variations. Sci Rep. 2018; 8: 1–10. https://doi.org/10.1038/s41598-017-17765-5 PMID: 29311619
5. Dessie Gessesse. Favouring a Demonised Plant Khat and Ethiopian smallholder-enterprises. Nordiska Afrikainstitutet, Uppsala, Sweden; 2013. Available: http://www.diva-portal.org/smash/record.jsf?pid=diva2:586499
6. Wuletaw M. Public discourse on Khat (Catha edulis) production in Ethiopia: Review. J Agric Ext Rural Dev. 2018; 10: 192–201. https://doi.org/10.5897/jaerd2018.0984
7. El Achaby M, El Miri N, Hannache H, Gmouh S, Ben youcef H, Aboulkas A. Production of cellulose nanocrystals from vine shoots and their use for the development of nanocomposite materials. Int J Biol Macromol. 2018; 117: 592–600. https://doi.org/10.1016/j.ijbiomac.2018.05.201 PMID: 29852228
8. Poletto M, Ornaghi Júnior HL, Zattera AJ. Native cellulose: Structure, characterization and thermal properties. Materials (Basel). 2014; 7: 6105–6119. https://doi.org/10.3390/ma7096105 PMID: 28788179
9. Gabriel T, Belete A, Syrowatka F, Neubert RHH, Gebre-Mariam T. Extraction and characterization of celluloses from various plant byproducts. Int J Biol Macromol. 2020; 158: 1248–1258. https://doi.org/10.1016/j.ijbiomac.2020.04.264 PMID: 32437811
10. Du H, Liu W, Zhang M, Si C, Zhang X, Li B. Cellulose nanocrystals and cellulose nanofibrils based hydrogels for biomedical applications. Carbohydr Polym. 2019; 209: 130–144. https://doi.org/10.1016/j.carbpol.2019.01.020 PMID: 30732792
11. Abitbol T, Rivkin A, Cao Y, Nevo Y, Abraham E, Ben-Shalom T, et al. Nanocellulose, a tiny fiber with huge applications. Curr Opin Biotechnol. 2016; 39: 76–88. https://doi.org/10.1016/j.copbio.2016.01.002 PMID: 26930621
12. Xiao Y, Liu Y, Wang X, Li M, Lei H, Xu H. Cellulose nanocrystals prepared from wheat bran: Characterization and cytotoxicity assessment. Int J Biol Macromol. 2019; 140: 225–233. https://doi.org/10.1016/j.ijbiomac.2019.08.160 PMID: 31437495
13. Klemm D, Cranston ED, Fischer D, Gama M, Kedzior SA, Kralisch D, et al. Nanocellulose as a natural source for groundbreaking applications in materials science: Today's state. Mater Today. 2018; 21: 720–748. https://doi.org/10.1016/j.mattod.2018.02.001
14. Wijaya CJ, Saputra SN, Soetaredjo FE, Putro JN, Lin CX, Kurniawan A, et al. Cellulose nanocrystals from passion fruit peels waste as antibiotic drug carrier. Carbohydr Polym. 2017; 175: 370–376. https://doi.org/10.1016/j.carbpol.2017.08.004 PMID: 28917878
15. Agarwal J, Mohanty S, Nayak SK. Valorization of pineapple peel waste and sisal fiber: Study of cellulose nanocrystals on polypropylene nanocomposites. J Appl Polym Sci. 2020; 137: 1–19. https://doi.org/10.1002/app.49291

16. Bettaieb F, Khiari R, Hassan ML, Belgacem MN, Bras J, Dufresne A, et al. Preparation and characterization of new cellulose nanocrystals from marine biomass Posidonia oceanica. Ind Crops Prod. 2015; 72: 175–182. https://doi.org/10.1016/j.indcrop.2014.12.038

17. Bettaieb F, Khiari R, Dufresne A, Mhenni MF, Belgacem MN. Mechanical and thermal properties of Posidonia oceanica cellulose nanocrystal reinforced polymer. Carbohydr Polym. 2015; 123: 99–104. https://doi.org/10.1016/j.carbpol.2015.01.026 PMID: 25843839

18. Benito-González I, López-Rubio A, Gavara R, Martínez-Sanz M. Cellulose nanocrystal-based films produced by more sustainable extraction protocols from Posidonia oceanica waste biomass. Cellulose. 2019; 26: 8007–8024. https://doi.org/10.1007/s10570-019-02641-4

19. Kallel F, Bettaieb F, Khiari R, García A, Bras J, Chaabouni SE. Isolation and structural characterization of cellulose nanocrystals extracted from garlic straw residues. Ind Crops Prod. 2016; 87: 287–296. https://doi.org/10.1016/j.indcrop.2016.04.060

20. Liu Z, Li X, Xie W, Deng H. Extraction, isolation and characterization of nanocrystalline cellulose from industrial kelp (Laminaria japonica) waste. Carbohydr Polym. 2017; 173: 353–359. https://doi.org/10.1016/j.carbpol.2017.05.079 PMID: 28732876

21. Danial WH, Mohd Taib R, Abu Samah MA, Mohd Salim R, Abdul Majid Z. The valorization of municipal grass waste for the extraction of cellulose nanocrystals. RSC Adv. 2020; 10: 42400–42407. https://doi.org/10.1039/d0ra07972c

22. Kanai N, Honda T, Yoshihara N, Oyama T, Naito A, Ueda K, et al. Structural characterization of cellulose nanofibers isolated from spent coffee grounds and their composite films with poly(vinyl alcohol): a new non-wood source. Cellulose. 2020; 27: 5017–5028. https://doi.org/10.1007/s10570-020-03113-w

23. Du H, Parit M, Wu M, Che X, Wang Y, Zhang M, et al. Sustainable valorization of paper mill sludge into cellulose nanofibrils and cellulose nanopaper. J Hazard Mater. 2020; 400: 123106. https://doi.org/10.1016/j.jhazmat.2020.123106 PMID: 32580093

24. Kumar V, Pathak P, Bhardwaj NK. Waste paper: An underutilized but promising source for nanocellulose mining. Waste Manag. 2020; 102: 281–303. https://doi.org/10.1016/j.wasman.2019.10.041 PMID: 31704510

25. Jackson JK, Letchford K, Wasserman BZ, Ye L, Hamad WY, Burt HM. The use of nanocrystalline cellulose for the binding and controlled release of drugs. Int J Nanomedicine. 2011; 6: 321–330. https://doi.org/10.2147/IJN.S16749 PMID: 21383857

26. Xu Q, Ji Y, Sun Q, Fu Y, Xu Y, Jin L. Fabrication of cellulose nanocrystal/chitosan hydrogel for controlled drug release. Nanomaterials. 2019;9. https://doi.org/10.3390/nano9020253 PMID: 30781761

27. Plackett D, Letchford K, Jackson J, Burt H. A review of nanocellulose as a novel vehicle for drug delivery. Nord Pulp Pap Res J. 2014; 29: 105–118. https://doi.org/10.3183/npprj-2014-29-01-p105-118

28. Lankalapalli S, Kolapalli RM. Biopharmaceutical evaluation of diclofenac sodium controlled release tablets prepared from gum karaya-chitosan polyelectrolyte complexes. Drug Dev Ind Pharm. 2012; 38: 815–824. https://doi.org/10.3109/03639045.2011.630006 PMID: 22087874

29. Bolla PK, Clark BA, Juluri A, Cheruvu HS, Renukuntla J. Evaluation of formulation parameters on permeation of ibuprofen from topical formulations using Strat-M® membrane. Pharmaceutics. 2020;12. https://doi.org/10.3390/pharmaceutics12020151 PMID: 32069850

30. de Oliveira JP, Bruni GP, el Halal SLM, Bertoldi FC, Dias ARG, Zavareze E da R. Cellulose nanocrystals from rice and oat husks and their application in aerogels for food packaging. Int J Biol Macromol. 2019; 124: 175–184. https://doi.org/10.1016/j.ijbiomac.2018.11.205 PMID: 30471399

31. Coelho CCS, Michelin M, Cerqueira MA, Gonçalves C, Tonon R V., Pastrana LM, et al. Cellulose nanocrystals from grape pomace: production, properties and cytotoxicity assessment. Carbohydr Polym. 2018; 192: 327–336. https://doi.org/10.1016/j.carbpol.2018.03.023 PMID: 29691028

32. Gong J, Mo L, Li J. A comparative study on the preparation and characterization of cellulose nanocrystals with various polymorphs. Carbohydr Polym. 2018; 195: 18–28. https://doi.org/10.1016/j.carbpol.2018.04.039 PMID: 29804966

33. Bano S, Negi YS. Studies on cellulose nanocrystals isolated from groundnut shells. Carbohydr Polym. 2017; 157: 1041–1049. https://doi.org/10.1016/j.carbpol.2016.10.069 PMID: 27987804

34. Abdel-Halim ES. Chemical modification of cellulose extracted from sugarcane bagasse: Preparation of hydroxyethyl cellulose. Arab J Chem. 2014; 7: 362–371. https://doi.org/10.1016/j.arabjc.2013.05.006

35. Yeasmin MS, Mondal MIH. Synthesis of highly substituted carboxymethyl cellulose depending on cellulose particle size. Int J Biol Macromol. 2015; 80: 725–731. https://doi.org/10.1016/j.ijbiomac.2015.07.040 PMID: 26210036

36. Lin L, Yan R, Liu Y, Jiang W. In-depth investigation of enzymatic hydrolysis of biomass wastes based on three major components: Cellulose, hemicellulose and lignin. Bioresour Technol. 2010; 101: 8217–8223. https://doi.org/10.1016/j.biortech.2010.05.084 PMID: 20639116

37. Smyth M, García A, Rader C, Foster EJ, Bras J. Extraction and process analysis of high aspect ratio cellulose nanocrystals from corn (Zea mays) agricultural residue. Ind Crops Prod. 2017; 108: 257–266. https://doi.org/10.1016/j.indcrop.2017.06.006

38. EP. Cellulose, Powdered. 8th ed. European Pharmacopoeia–State Of Work Of Pharmeuropa, Harmonisation. Healthcare, European Directorate for the Quality of Medicines and International, (EDQM).; 2013.

39. Popescu M, Popescu C, Lisa G, Sakata Y. Evaluation of morphological and chemical aspects of different wood species by spectroscopy and thermal methods. J Mol Struct. 2011; 988: 65–72. https://doi.org/10.1016/j.molstruc.2010.12.004

40. Aguayo MG, Pérez AF, Reyes G, Oviedo C, Gacitúa W, Gonzalez R, et al. Isolation and characterization of cellulose nanocrystals from rejected fibers originated in the Kraft Pulping process. Polymers (Basel). 2018; 10: 1145–1156. https://doi.org/10.3390/polym10101145 PMID: 30961070

41. Gabriel T, Belete A, Gebre-Mariam T. Preparation and evaluation of carboxymethyl enset and cassava starches as pharmaceutical gelling agents. J Drug Deliv Ther. 2013; 3: 1–10.

42. Ubaid M, Ilyas S, Mir S, Khan AK, Rashid R. Formulation and in vitro evaluation of carbopol 934-based modified clotrimazole gel for topical application. An Acad Bras Cienc. 2016; 88: 2303–2317. https://doi.org/10.1590/0001-3765201620160162 PMID: 27925034

43. Aiyalu R, Govindarjan A, Ramasamy A. Formulation and evaluation of topical herbal gel for the treatment of arthritis in animal model. Brazilian J Pharm Sci. 2016; 52: 493–507. https://doi.org/10.1590/s1984-82502016000300015

44. Dantas MGB, Reis SAGB, Damasceno CMD, Rolim LA, Rolim-Neto PJ, Carvalho FO, et al. Development and Evaluation of Stability of a Gel Formulation Containing the Monoterpene Borneol. Sci World J. 2016; 2016: 1–4. https://doi.org/10.1155/2016/7394685 PMID: 27247965

45. Kittipongpatana OS, Burapadaja S, Kittipongpatana N. Carboxymethyl mungbean starch as a new pharmaceutical gelling agent for topical preparation. Drug Dev Ind Pharm. 2009; 35: 34–42. https://doi.org/10.1080/03639040802144229 PMID: 18720150

46. Jahan MS, Saeed A, He Z, Ni Y. Jute as raw material for the preparation of microcrystalline cellulose. Cellulose. 2011; 18: 451–459. https://doi.org/10.1007/s10570-010-9481-z

47. Nuruddin M, Chowdhury A, Haque SA, Rahman M, Farhad SF, Jahan MS, et al. Extraction and characterization of cellulose microfibrils from agricultural wastes in an integrated biorefinery initiative. Cellul Chem Technol. 2011; 45: 347–354.

48. Watkins D, Nuruddin M, Hosur M, Tcherbi-Narteh A, Jeelani S. Extraction and characterization of lignin from different biomass resources. J Mater Res Technol. 2015; 4: 26–32. https://doi.org/10.1016/j.jmrt.2014.10.009

49. Candido RG, Gonçalves AR. Synthesis of cellulose acetate and carboxymethylcellulose from sugarcane straw. Carbohydr Polym. 2016; 152: 679–686. https://doi.org/10.1016/j.carbpol.2016.07.071 PMID: 27516319

50. PhEur. Cellulose powder. 8th ed. European Pharmacopoeia. 8th ed. Strasbourg, France: European Directorate for the Quality of Medicines & HealthCare (EDQM) and Council of Europe; 2013. http://pharmeuropa.edqm.eu

51. Alghooneh A, Mohammad Amini A, Behrouzian F, Razavi SMA. Characterisation of cellulose from coffee silverskin. Int J Food Prop. 2017; 20: 2830–2843. https://doi.org/10.1080/10942912.2016.1253097

52. Golbaghi L, Khamforoush M, Hatami T. Carboxymethyl cellulose production from sugarcane bagasse with steam explosion pulping: Experimental, modeling, and optimization. Carbohydr Polym. 2017; 174: 780–788. https://doi.org/10.1016/j.carbpol.2017.06.123 PMID: 28821131

53. Abd El-Fattah M, Hasan AMA, Keshawy M, El Saeed AM, Aboelenien OM. Nanocrystalline cellulose as an eco-friendly reinforcing additive to polyurethane coating for augmented anticorrosive behavior. Carbohydr Polym. 2018; 183: 311–318. https://doi.org/10.1016/j.carbpol.2017.12.084 PMID: 29352890

54. Meng F, Zhang X, Yu W, Zhang Y. Kinetic analysis of cellulose extraction from banana pseudo-stem by liquefaction in polyhydric alcohols. Ind Crops Prod. 2019; 137: 377–385. https://doi.org/10.1016/j.indcrop.2019.05.025

55. Tsegaye B, Balomajumder C, Roy P. Alkali pretreatment of wheat straw followed by microbial hydrolysis for bioethanol production. Environ Technol (United Kingdom). 2019; 40: 1203–1211. https://doi.org/10.1080/09593330.2017.1418911 PMID: 29251554

56. Mariano M, Cercená R, Soldi V. Thermal characterization of cellulose nanocrystals isolated from sisal fibers using acid hydrolysis. Ind Crops Prod. 2016; 94: 454–462. https://doi.org/10.1016/j.indcrop.2016.09.011

57. Zhang H, Chen Y, Wang S, Ma L, Yu Y, Dai H, et al. Extraction and comparison of cellulose nanocrystals from lemon (Citrus limon) seeds using sulfuric acid hydrolysis and oxidation methods. Carbohydr Polym. 2020; 238: 116180. https://doi.org/10.1016/j.carbpol.2020.116180 PMID: 32299561

58. Collazo-Bigliardi S, Ortega-Toro R, Chiralt Boix A. Isolation and characterisation of microcrystalline cellulose and cellulose nanocrystals from coffee husk and comparative study with rice husk. Carbohydr Polym. 2018; 191: 205–215. https://doi.org/10.1016/j.carbpol.2018.03.022 PMID: 29661311

59. García-García D, Balart R, Lopez-Martinez J, Ek M, Moriana R. Optimizing the yield and physico-chemical properties of pine cone cellulose nanocrystals by different hydrolysis time. Cellulose. 2018; 25: 2925–2938. https://doi.org/10.1007/s10570-018-1760-0

60. Xing L, Gu J, Zhang W, Tu D, Hu C. Cellulose I and II nanocrystals produced by sulfuric acid hydrolysis of Tetra pak cellulose I. Carbohydr Polym. 2018; 192: 184–192. https://doi.org/10.1016/j.carbpol.2018.03.042 PMID: 29691011

61. Haafiz MKM, Hassan A, Zakaria Z, Inuwa IM. Isolation and characterization of cellulose nanowhiskers from oil palm biomass microcrystalline cellulose. Carbohydr Polym. 2014; 103: 119–125. https://doi.org/10.1016/j.carbpol.2013.11.055 PMID: 24528708

62. Meng F, Wang G, Du X, Wang Z, Xu S, Zhang Y. Extraction and characterization of cellulose nanofibers and nanocrystals from liquefied banana pseudo-stem residue. Compos Part B Eng. 2019; 160: 341–347. https://doi.org/10.1016/j.compositesb.2018.08.048

63. Rosa MF, Medeiros ES, Malmonge JA, Gregorski KS, Wood DF, Mattoso LHC, et al. Cellulose nanowhiskers from coconut husk fibers: Effect of preparation conditions on their thermal and morphological behavior. Carbohydr Polym. 2010; 81: 83–92. https://doi.org/10.1016/j.carbpol.2010.01.059

64. Xie J, Hse CY, De Hoop CF, Hu T, Qi J, Shupe TF. Isolation and characterization of cellulose nanofibers from bamboo using microwave liquefaction combined with chemical treatment and ultrasonication. Carbohydr Polym. 2016; 151: 725–734. https://doi.org/10.1016/j.carbpol.2016.06.011 PMID: 27474619

65. Yang H, Yan R, Chen H, Lee DH, Zheng C. Characteristics of hemicellulose, cellulose and lignin pyrolysis. Fuel. 2007; 86: 1781–1788. https://doi.org/10.1016/j.fuel.2006.12.013

66. Mohamad Haafiz MK, Eichhorn SJ, Hassan A, Jawaid M. Isolation and characterization of microcrystalline cellulose from oil palm biomass residue. Carbohydr Polym. 2013; 93: 628–634. https://doi.org/10.1016/j.carbpol.2013.01.035 PMID: 23499105

67. Tarchoun AF, Trache D, Klapötke TM. Microcrystalline cellulose from Posidonia oceanica brown algae: Extraction and characterization. Int J Biol Macromol. 2019; 138: 837–845. https://doi.org/10.1016/j.ijbiomac.2019.07.176 PMID: 31356946

68. Singh S, Gaikwad KK, Park S II, Lee YS. Microwave-assisted step reduced extraction of seaweed (Gelidiella aceroso) cellulose nanocrystals. Int J Biol Macromol. 2017; 99: 506–510. https://doi.org/10.1016/j.ijbiomac.2017.03.004 PMID: 28267615

69. Prado KS, Spinacé MAS. Isolation and characterization of cellulose nanocrystals from pineapple crown waste and their potential uses. Int J Biol Macromol. 2019; 122: 410–416. https://doi.org/10.1016/j.ijbiomac.2018.10.187 PMID: 30385342

70. Wang Z, Yao Z, Zhou J, He M, Jiang Q, Li S, et al. Isolation and characterization of cellulose nanocrystals from pueraria root residue. Int J Biol Macromol. 2019; 129: 1081–1089. https://doi.org/10.1016/j.ijbiomac.2018.07.055 PMID: 30009914

71. Wada M, Okano T. Localization of Iα and Iβ phases in algal cellulose revealed by acid treatments. Cellulose. 2001; 8: 183–188. https://doi.org/10.1023/A:1013196220602

72. Kim UJ, Eom SH, Wada M. Thermal decomposition of native cellulose: Influence on crystallite size. Polym Degrad Stab. 2010; 95: 778–781. https://doi.org/10.1016/j.polymdegradstab.2010.02.009

73. Nuruddin M, Hosur M, Uddin MJ, Baah D, Jeelani S. A novel approach for extracting cellulose nanofibers from lignocellulosic biomass by ball milling combined with chemical treatment. J Appl Polym Sci. 2016; 133: 1–10. https://doi.org/10.1002/app.42990

74. Morán JI, Alvarez VA, Cyras VP, Vázquez A. Extraction of cellulose and preparation of nanocellulose from sisal fibers. Cellulose. 2008; 15: 149–159. https://doi.org/10.1007/s10570-007-9145-9

75. Thomas D, Latha MS, Thomas KK. Synthesis and in vitro evaluation of alginate-cellulose nanocrystal hybrid nanoparticles for the controlled oral delivery of rifampicin. J Drug Deliv Sci Technol. 2018; 46: 392–399. https://doi.org/10.1016/j.jddst.2018.06.004

76. Benini KCC de C, Voorwald HJC, Cioffi MOH, Rezende MC, Arantes V. Preparation of nanocellulose from Imperata brasiliensis grass using Taguchi method. Carbohydr Polym. 2018; 192: 337–346. https://doi.org/10.1016/j.carbpol.2018.03.055 PMID: 29691029

77. Stinson-Bagby KL, Roberts R, Foster EJ. Effective cellulose nanocrystal imaging using transmission electron microscopy. Carbohydr Polym. 2018; 186: 429–438. https://doi.org/10.1016/j.carbpol.2018.01.054 PMID: 29456006

78. Silvério HA, Flauzino Neto WP, Dantas NO, Pasquini D. Extraction and characterization of cellulose nanocrystals from corncob for application as reinforcing agent in nanocomposites. Ind Crops Prod. 2013; 44: 427–436. https://doi.org/10.1016/j.indcrop.2012.10.014

79. Rhim JW, Reddy JP, Luo X. Isolation of cellulose nanocrystals from onion skin and their utilization for the preparation of agar-based bio-nanocomposites films. Cellulose. 2015; 22: 407–420. https://doi.org/10.1007/s10570-014-0517-7

80. Patel NA, Patel NJ, Patel RP. Formulation and valuation of curcumin gel for topical application. Pharm Dev Technol. 2009; 14: 83–92. https://doi.org/10.1080/10837450802409438